Available online at www.sciencedirect.com
ScienceDirect
Ceramics International 37 (2011) 1301–1306
CERAMICS INTERNATIONAL
www.elsevier.com/locate/ceramint

Chemical vapor deposition and composition–depth profiling of a graded coating by Auger electron spectroscopy used in conjunction with taper polishing

S. Eroglu *, B. Gallois

Stevens Institute of Technology, Dept. of Chemical and Materials Eng., Hoboken, NJ, USA

Received 19 February 2010; received in revised form 29 November 2010; accepted 6 December 2010
Available online 21 January 2011

Abstract

A graded TiC_xN_{1-x} coating with x varying parabolically in the range 0–1 was grown by chemical vapor deposition in the $TiCL_4$–CH_4–N_2–H_2 system by quasi-continuously changing process parameters (growth time, CH_4 mole fraction) at 1400 K and at 10.7 kPa. Taper polishing of the graded coating was carried out by a simple apparatus converting a depth dimension into a lateral dimension. Auger electron spectroscopy line scan was then performed on the taper polished surface. Composition profile of the graded coating was determined to be in agreement with the designed one using surface profilometer traces and AES signals from C_{KLL} transition at 272 eV. AES/taper polishing approach facilitates composition–depth analysis with a minimal degree of sputtering and a substantial reduction of data acquisition time. Taper polishing could also be combined with other chemical analysis techniques such as X-ray microdiffraction.

Keywords: B. Electron microscopy; D. Carbides; D. Nitrides; Chemical vapor deposition

1. Introduction

In many monolithic coating/substrate systems, the transition from the substrate to the coating usually involves an abrupt change in composition and in properties such as thermal expansion coefficient, hardness or thermal conductivity. Stresses are inevitably produced in the interfacial region during cooling from the deposition temperature or during service. These stresses can affect the integrity of the coating/substrate system. By continuously changing the composition of the coating, a close match between properties may be obtained at the substrate/coating interface. Since the properties change gradually from the substrate to the surface layer, stresses induced during cooling from the deposition temperature or during service are reduced and not localized at the interface. Thus, adhesion and cohesion of the coating can be improved leading to increased life time of the coating/substrate composite. Within this concept, functionally graded materials (FGMs) or coatings seem to be a promising alternative to conventional materials. FGMs were born in Japan in mid-1980s in association with the development heat-shielding structural materials [1]. Excellent reviews of FGMs are given in Refs. [2,3]. The techniques for fabrication of functionally graded materials include chemical vapor deposition (CVD), physical vapor deposition, plasma spray, powder metallurgy and sol–gel techniques [4–9].

TiC_xN_{1-x} coatings deposited on WC/Co, graphite and steel by CVD have been used in many areas ranging from cutting tools to nuclear materials owing to high hardness, superior inertness and low Z-number. In our previous works [10,11], chemical vapor deposition of monolithic and graded Ti_xCN_{1-x} coatings with linear and exponential concentration profiles were reported. In these studies, important details of compositional analysis have, however, remained obscure. Hence, the current work was undertaken to give detailed description of taper polishing, surface profile tracing and Auger electron spectroscopy (AES) techniques used for composition–depth studies. In order to accomplish this, TiC_xN_{1-x} coating with x

* Corresponding author. Present address: Istanbul University, Engineering Faculty, Dept. of Metallurgical and Materials Eng., Avcılar, Turkey.
Tel.: +90 212 473 7065; fax: +90 212 473 7180.
E-mail address: serafettine63@gmail.com (S. Eroglu).

0272-8842/$36.00
doi:10.1016/j.ceramint.2010.12.001

varying parabolically in the range 0–1 with thickness was grown by chemical vapor deposition. The structural development of the coating and possible artifacts of the composition profiling by the combined techniques were also discussed.

2. Experimental procedures

2.1. Chemical vapor deposition

Fig. 1 shows schematic presentation of the hot-wall CVD reactor employed for the growth of the graded coating. The reactor consisted of the reactant supply system, the reaction chamber, the vacuum station and the computer interface. The entire CVD system was controlled using a computer to which various process controllers and valves were interfaced. The reaction chamber was heated by a tubular furnace. A wedge shaped sample holder was mounted on a quartz tube which would be rapidly retracted into the cold region using magnetic clutch to reduce further reaction. The substrate material was electronic grade graphite. Graphite substrate was used because it is an important material widely employed in many areas ranging from nuclear to aerospace industries. TiC_xN_{1-x} coatings improve surface characteristics of graphite such as resistance to oxidation at high temperatures and erosion by particles and gas streams. The reactant gases, namely, hydrogen, methane, nitrogen and argon of ultrahigh purity (99.9995) were used. The reactant supply system was equipped with mass flow controllers paired with compressed air fast acting valves. The $TiCl_4$ vapor, a titanium source, was carried from the bubbler heated in an oil bath, with the flow of H_2 carrier gas. The chemical vapor deposition was carried out using total gas ($CH_4 + N_2 + H_2 + TiCl_4$) flow rate of 670 cm^3/min, $CH_4 + N_2$ flow rate of 175 cm^3/min and $TiCl_4$ flow rate of 20 cm^3/min at 1400 K and at a reduced pressure of 10.7 kPa. For the growth of graded coating, all parameters were kept constant, but the ratio of CH_4 flow rate to $CH_4 + N_2$ flow rate (CH_4 mole fraction) was varied from zero to unity as the growth proceeded.

The parabolic grading function of $C_x = aZ^2 + bZ + c$ was selected for the present study, where C_x is the desired composition (TiC mole fraction) at distance Z from the start of the graded coating and a, b and c are boundary depended coefficients. A parabolic grading function was selected because our previous work [12] showed that growth of the parabolically graded coating resulted in compressive stress (−500 MPa) in the coating which prevents crack formation. For the parabolically graded coating with $C_x = 0$ at $Z = 0$ and $C_x = 1$ at $Z = 22$ μm, the boundary coefficients are $a = 1/484$, $b = 0$ and $c = 0$. The coating is divided into 21 layers of constant composition with an increment of 0.05 which is achievable by the quasi-continuous variation of reactant (CH_4 and N_2) flow rates. Growth time and reactant flow rates for each layer were calculated up to 21st layer in accordance with the methodology described in our previous work [11]. The data generated for the chemical vapor deposition of the parabolically graded coating is shown in Fig. 2. The growth of the coating was carried out in short time steps of constant methane mole fraction specified for each layer. In order to provide clear delineation of the graded coating, TiN with a thickness of 6 μm was first deposited on the substrate. The graded material was then deposited on this layer

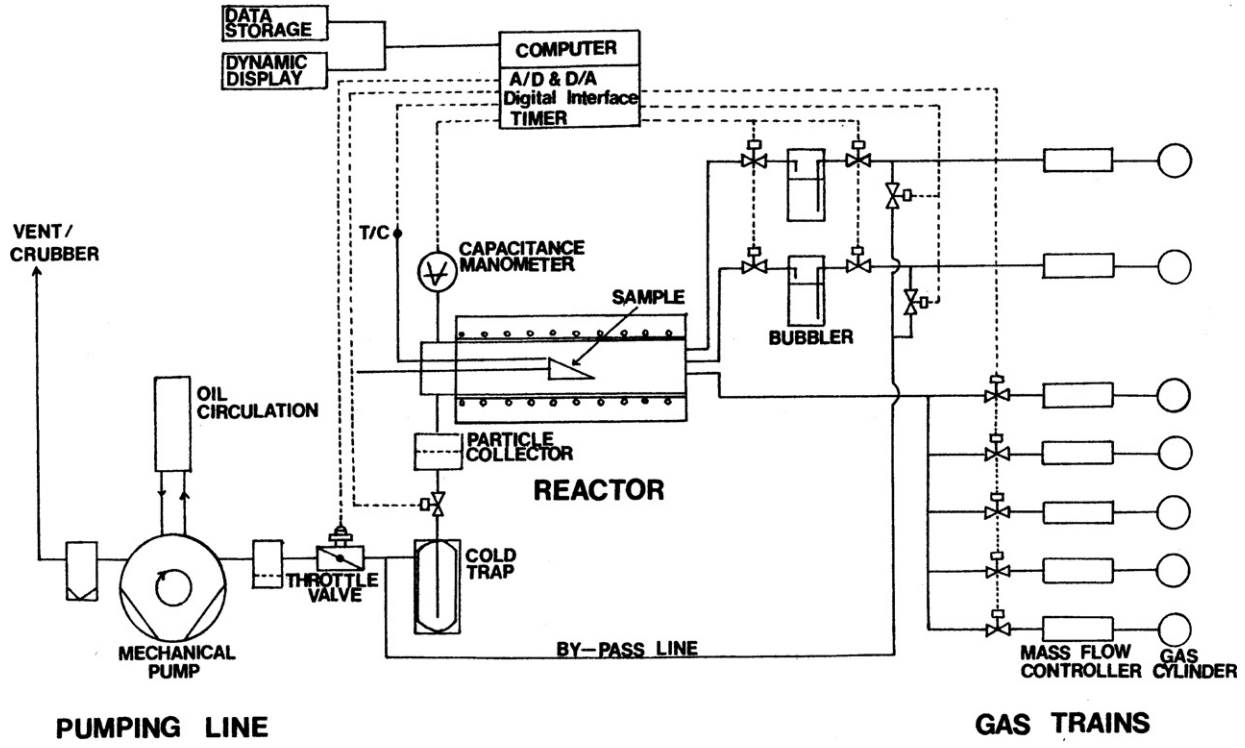

Fig. 1. Schematic illustration of the chemical vapor deposition system.

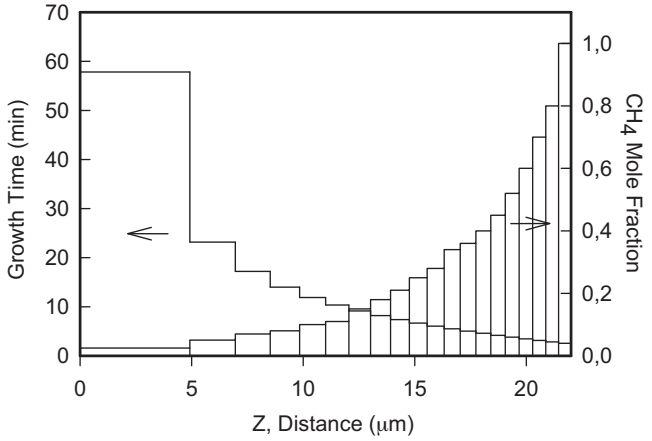

Fig. 2. Growth time and CH_4 mole fraction specified for each layer that will produce a parabolically graded coating. CH_4 mole fraction is defined as $CH_4/(CH_4 + N_2)$ where $CH_4 + N_2$ flow rate is 175 cm^3/min.

and was followed by a final layer of TiC 10 μm thick. The graded zone had a thickness of 22 μm.

Morphology of the coating was examined in a JEOL Scanning electron microscope (Model JSM-840). The coated sample was broken in the middle into two pieces for the cross-sectional examination and composition–depth analysis. The thickness of the unpolished coating was determined from the micrograph of the cross section.

2.2. Composition–depth profiling

Scanning Auger electron microscopy was used to determine composition–depth profile of the graded coating. Since conventional profiling by sputtering is slow for thick coatings, an alternative approach was to produce a taper section [13], thus exposing the subsurface regions of the coating (converting a depth dimension into a lateral dimension). This was accomplished by a device shown schematically in Fig. 3. The device consisted of two cemented carbide inserts mounted on either side of an aluminum block with dissimilar heights to produce a height gradient sufficient to achieve a lapping angle of 2.5° with respect to the coating surface. The sample was mounted on a sample holder located between the two carbide

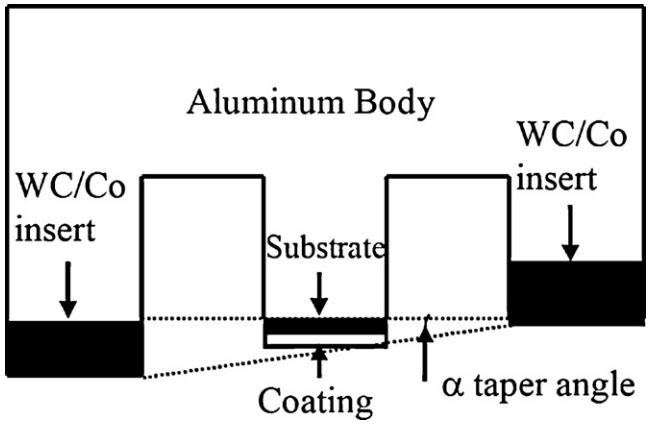

Fig. 3. Schematic picture of the apparatus used for taper polishing.

inserts. Mechanical lapping was performed using 1-μm diamond paste fed on a nylon polishing cloth on a rotating wheel. Further lapping was conducted on the nylon cloth without diamond paste in order to obtain a mirror-like surface. Occasionally, the sample was examined under optical microscope to see degree of polishing. The quality and extent of taper polishing were also checked by a Dektak Profilometer. When the coating/substrate interface was reached, polishing was stopped.

The procedure for the determination of composition–depth profile of the coating can be explained schematically with the help of Fig. 4. The taper polished sample is displayed in Fig. 4a where the line marked ABCD extends from the horizontal surface through tapered surface to the leading edge on the right. The surface profile along the ABCD line was determined by a Dektak profilometer. A sharp stylus was placed in contact with the horizontal surface, and then gently dragged along the surface until the leading edge was reached. The resultant profilometer trace is shown schematically in Fig. 4b (upper sketch). The vertical deflection measures the depth from the original surface or the distance from the coating/substrate interface. The linear region in the trace and the leading edge were taken as references for the depth and horizontal distance, respectively.

The sample was introduced to a Perkin-Elmer Physical Electronics scanning Auger electron spectrometer. The elemental horizontal scans were conducted by scanning the electron beam across the coating along the line of ABCD. Care was taken to ensure that the scanned line was close to the one revealed by the profilometer. The line scan resulted in an Auger intensity profile as a function of horizontal distance traveled (lower sketch in Fig. 4b).

To obtain composition profile, the depth or the distance from interface was measured from the trace (upper sketch) for a given horizontal distance and the corresponding intensity data was recorded from the horizontal Auger line scan (lower sketch). This treatment was carried out at numerous positions along the ABCD line. AES intensity data obtained was then plotted against the depth or the distance from the interface (Fig. 4c). This procedure minimizes the errors due to edge rounding, which occurs during metallographic polishing.

Surface contamination in the sample surface was removed prior to AES analysis by sputter cleaning with 3 keV argon ions for 3 min. The electron beam energy was 3 keV with a 0.005 μA beam current. The diameter of the electron beam was equal to be 20 μm. Because the nitrogen peak (383 eV) overlaps with the titanium peak (387 eV), only line scans for the carbon peak (KLL Auger transition at 272 eV) were performed.

3. Results and discussion

Fig. 5 shows the cross-sectional view (fractured surface) of the unpolished coating. The total thickness is determined to be 36 μm, in reasonable agreement with the theoretical thickness of 38 μm. The morphology of the coating consists of fine grains near the interface between the coating and substrate. It is

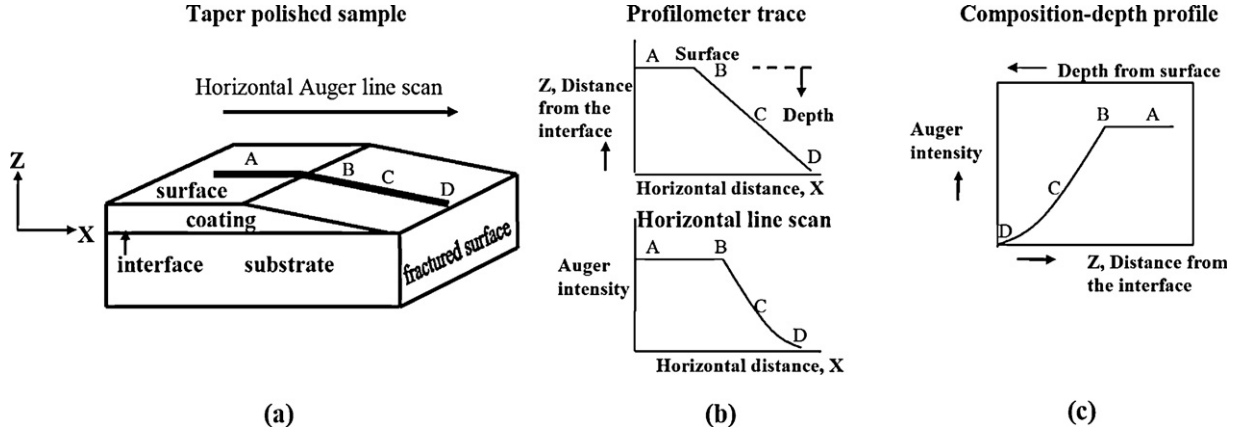

Fig. 4. Schematic illustration of composition–depth profiling by scanning Auger spectrometer used in conjunction with taper polishing. (a) Taper polished sample; (b) upper and lower sketches show profilometer trace and Auger intensity as a function of horizontal distance, respectively; (c) combined output of those in (b) represent the Auger intensity as a function of depth or distance from the interface.

apparent that the change in the reactant gas composition does not lead to nucleation of new grains at distances >20 μm where large columnar grains appear. Fine grains with a favorable crystallographic orientation were survived into large columnar ones as the growth proceeded. X-ray diffraction peak intensities from the top TiC layer showed that the growth of the grains with a ⟨1 0 0⟩ orientation perpendicular to the surface is preferred. It is suggested that graded layers grow epitactically on each other owing to the complete miscibility in the TiC–TiN system with fcc structure of NaCl [14].

Fig. 6 shows the profilometer trace of the taper polished sample. Surface profiling was started from the unpolished region which is characterized by horizontal linear trace. This region is followed by sloping trace which dropped at the leading edge of the sample. Since the thickness of the coating is known, the positions of the top TiC layer, graded zone, TiN layer and graphite substrate can be located in the trace as designated by the horizontal dashed lines in the figure. It is seen that the coating was nearly taper polished down to the interface. Trace rounding is also seen by the leading edge and in the top TiC layer. As deduced from the linear trace in the graded zone, the actual lapping angle is equal to be ∼1°, lower than theoretical one. Since graded zone has a thickness of ∼ 22 μm, the taper polishing provides a magnification of ∼60 or an equivalent length of 60 μm × 22 μm for the graded zone. This enables facile determination of compositional profile of the graded coating.

Fig. 7a shows Auger spectrum of the top TiC layer which reveals the characteristic shape of the peak due to the C_{KLL} Auger transition at 272 eV. The spectrum for the graphite substrate is also displayed in Fig. 7b for comparison. As seen from the figure, C_{KLL} peak at 272 eV from the TiC phase appears to be symmetrical, whereas the one from graphite is not. This observation suggests that the shape of the C peak is influenced by the changes in the local chemical environment.

The intensity of the AES signal in the form of peak-to-peak height, which is a function of relative concentration of the C element in the coating, was normalized to the maximum value (to that of pure TiC top layer). Fig. 8 displays the experimental carbon profile obtained by the Auger line scan combined with the profilometer trace. The designed profile is also shown in the figure. As can be seen from the figure, the coating starts with carbon intensity around ∼0.3 at ∼2 μm and it approaches zero at ∼8 μm, becomes nearly constant up to 12 μm and then increases with distance from the interface. The carbon intensity does not change above ∼29 μm, indicating the presence of the TiC layer. The graded zone is found to be in agreement with the

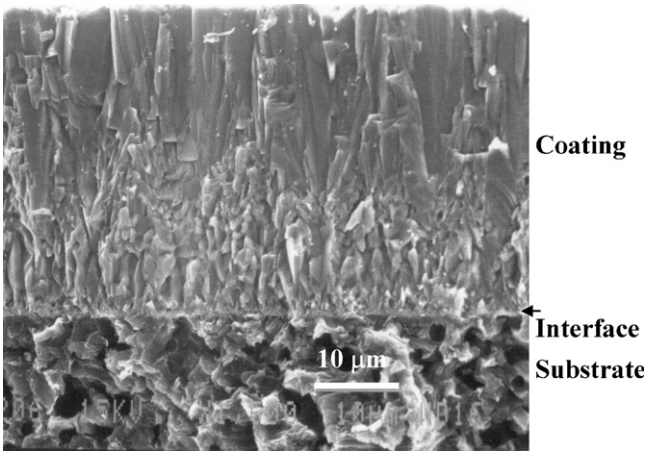

Fig. 5. SEM image of the cross section of the graded coating/substrate.

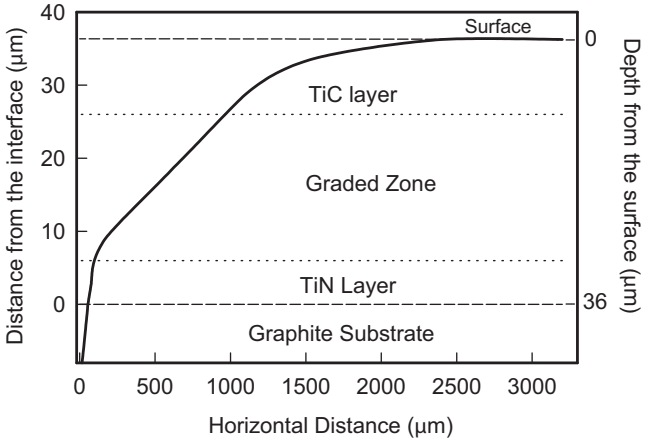

Fig. 6. Surface profilometer trace of the taper polished surface. Note that the origin of the horizontal distance is at the leading edge.

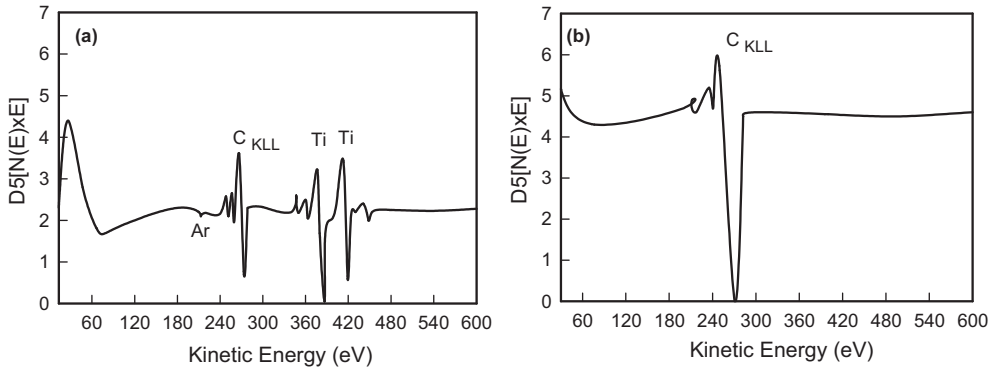

Fig. 7. Auger electron spectra of (a) TiC top layer and (b) graphite substrate.

designed curve. There is, however, scattered C signals in the region between 2 and 6 μm near the substrate are observed in the TiN layer, suggesting that line scans of tapered interfaces should be interpreted with caution. Preferential removal of softer TiN, graphite substrate protruding the TiN over layer (island effect), electron beam overlap at the graphite/TiN layer interface and embedded diamond particles into softer TiN layer may cause the random C signals seen at distances <6 μm in Fig. 8. It should be noted that scattered random C signals in TiN layer is not attributable to C diffusion from graphite substrate to TiN layer as studies on thin monolithic TiN coatings showed no TiC_xN_{1-x} phase. This was expected owing to sluggish solid state diffusion of C from the graphite substrate to the coating at 1400 K.

It should be mentioned that conventional depth profiling by traditional ion sputtering requires prolonged time. This introduces potential sputtering artifacts (varying removal of surface atoms, knock-on implantation, selective sputtering) that can generate false chemical/elemental concentration profiles. AES/taper polishing approach facilitates composition–depth analysis with a minimal degree of sputtering and a substantial reduction of data acquisition time over conventional depth profiling. Furthermore, it should be pointed out that taper polished surfaces of the samples with strong gradients in composition, stress and texture can be analyzed using other techniques such as relatively new X-ray microdiffraction which allows localized, spatially resolved measurements of the microstructural properties. For example, lattice constant in the Ti–C–N system varies linearly with composition (known as Vergard's law). With the microdiffraction from the taper polished surface, composition–depth profile can also be determined from the lattice constant measurements. The combined approach could also be extended to multiphase functionally graded coatings such as Ni/ZrO_2.

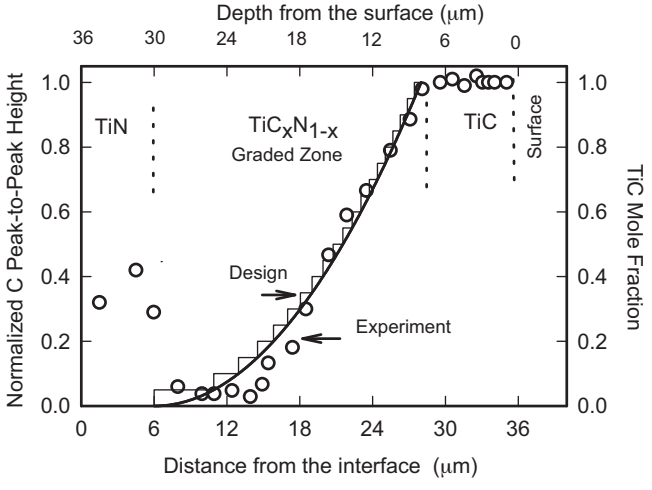

Fig. 8. Carbon profile of the graded coating deduced from horizontal line scan and profilometer trace.

4. Conclusions

A parabolically graded TiC_xN_{1-x} coating was grown by chemical vapor deposition by quasi-continuously varying process parameters (growth time, CH_4 and N_2 reactant flow rates) at 1400 K and at 0.1 atm. Taper polishing was applied to the coating using a simple polishing apparatus. This study shows the advantages of the AES used in conjunction with a taper sectioned coating. Increased lateral resolution with a minimum sputtering was achieved through the taper polishing/AES approach. The technique was successfully applied to the TiC_xN_{1-x} coating with parabolic composition–depth profile. It is suggested that taper polishing can also be used in combination with X-ray microdiffraction to reveal spatially resolved structural changes in functionally graded coatings.

Acknowledgements

The authors gratefully acknowledge the partial support of the Army Research Office, Division of Materials Science, under contact DAAG29-85-K-0124, and the New Jersey Advanced Technology Center for Surface Engineered Materials. S. Eroglu was partially supported by the Ministry of Education of the Republic of Turkey.

References

[1] Fabricating functionally gradient materials, Am. Ceram. Soc. Bull. 71 (4) (1992) 624–626.
[2] Y. Miamoto, W.A. Kaysser, B.H. Rabin, A. Kawasaki, R.G. Ford, Functionally Graded Materials: Design Processing and Applications, Kluwer Academic Publishers, Boston, London, 1999
[3] A. Mortensen, S. Suresh, Functionally graded metals and metal ceramic composites. Part 1. Processing, Int. Mater. Rev. 40 (1995) 239–265.

[4] E. Roos, K. Maile, K. Berreth, A. Lyutovich, R. Weiss, T. Perova, A. Moore, Chemical vapour deposition of PyC–Si_xC_y–SiC–Si_3N_4 multilayer with graded C···SiC transition, Surf. Coat. Technol. 180–181 (2004) 465–469.
[5] U. Schulz, M. Peters, Fr.-W. Bach, G. Tegeder, Graded coatings for thermal, wear and corrosion barriers, Mater. Sci. Eng. A 362 (2003) 61–80.
[6] V Cannillo, L. Lusvarghi, C. Siligardi, A. Sola, Effects of different production techniques on glass–alumina functionally graded materials, Ceram. Int. 34 (7) (2008) 1719–1727.
[7] S. Eroglu, N.C. Birla, M. Demirci, T. Baykara, Synthesis of functionally gradient NiCr–Al/MgO–ZrO_2 coatings by plasma spray technique, J. Mater. Sci. Lett. 12 (1993) 1099–1102.
[8] J. Li, X. Yao, Dependence of the properties of compositionally graded Pb(Zr, Ti)O_3 ferroelectric films of the bottom electrode, Ceram. Int. 34 (4) (2008) 1031–1034.
[9] A. Kawasaki, R. Watanabe, Concept and P/M fabrication of functionally gradient materials, Ceram. Int. 23 (1) (1997) 73–83.
[10] S. Eroglu, B. Gallois, Growth and structure of TiC_xN_y coatings chemically vapour deposited on graphite substrates, J. Mater. Sci. 32 (1997) 207–213.
[11] S. Eroglu, B. Gallois, Design and chemical vapor deposition of graded TiN/TiC coatings, Surf. Coat. Technol. 59 (1991) 275–278.
[12] S. Eroglu, B. Gallois, Residual stresses in chemically vapor deposited coatings in the Ti–C–N system, J. Phys. IV 3 (1993) 155–162.
[13] R.L. Moore, L. Salvati, G. Sundberg, V. Greenhut, Surface analysis of diffusion zones in multiple chemical vapor deposition coatings, J. Vac. Sci. Technol. A (3) (1985) 2426–2431.
[14] P. Duwez, F. Odell, Phase relationships in the binary systems of nitrides and carbides of zirconium, columbium, titanium, and vanadium, J. Electrochem. Soc. 97 (1950) 299–304.